AD-A148 203 CHARACTERIZATION OF III-V COMPOUND SEMICONDUCTOR DEVICE 1/1
MATERIALS(U) AIR FORCE WRIGHT AERONAUTICAL LABS
WRIGHT-PATTERSON AFB OH D C REYNOLDS MAY 84
UNCLASSIFIED AFWAL-TR-84-1032 F/G 20/12 NL

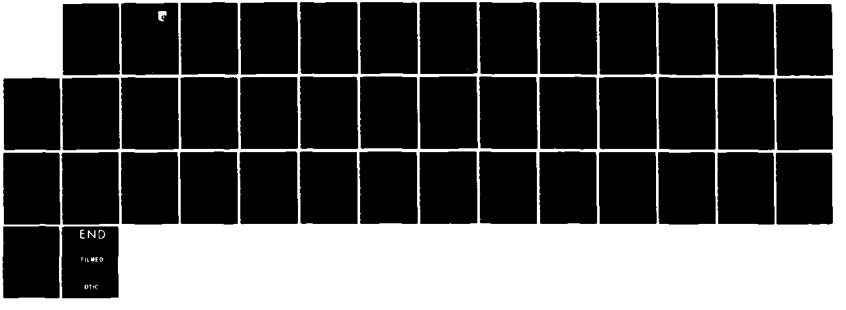

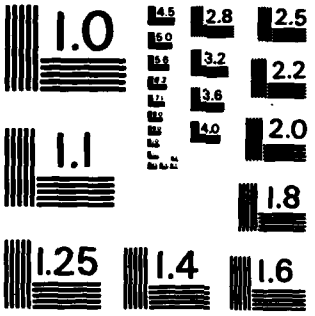

MICROCOPY RESOLUTION TEST CHART
NATIONAL BUREAU OF STANDARDS-1963-A

AFWAL-TR-84-1032

(1)

AD-A148 203

CHARACTERIZATION OF III-V COMPOUND SEMICONDUCTOR DEVICE MATERIALS

D. C. Reynolds
Electronic Research Branch
Electronic Technology Division

May 1984

Final Report for Period October 1979 - October 1983

Approved for public release; distribution unlimited.

DTIC FILE COPY

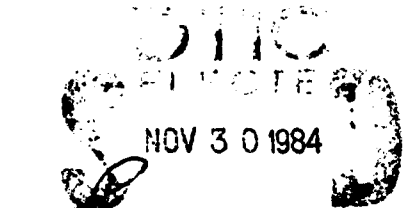

AVIONICS LABORATORY
AIR FORCE WRIGHT AERONAUTICAL LABORATORIES
AIR FORCE SYSTEMS COMMAND
WRIGHT-PATTERSON AIR FORCE BASE, OHIO 45433

84 11 26 189

NOTICE

When Government drawings, specifications, or other data are used for any purpose other than in connection with a definitely related Government procurement operation, the United States Government thereby incurs no responsibility nor any obligation whatsoever; and the fact that the government may have formulated, furnished, or in any way supplied the said drawings, specifications, or other data, is not to be regarded by implication or otherwise as in any manner licensing the holder or any other person or corporation, or conveying any rights or permission to manufacture, use, or sell any patented invention that may in any way be related thereto.

This technical report has been reviewed and is approved for publication.

D. C. REYNOLDS, Senior Scientist
Electronic Research Branch
Avionics Laboratory

FOR THE COMMANDER:

PHILIP E. STOVER, Chief
Electronic Research Branch
Avionics Laboratory

If your address has changed, if you wish to be removed from our mailing list, or if the addressee is no longer employed by your organization please notify AFWAL/AADR, W-P AFB, OH 45433 to help maintain a current mailing list.

Copies of this report should not be returned unless return is required by security considerations, contractual obligations, or notice on a specific document.

Unclassified

SECURITY CLASSIFICATION OF THIS PAGE *(When Data Entered)*

REPORT DOCUMENTATION PAGE	READ INSTRUCTIONS BEFORE COMPLETING FORM
1. REPORT NUMBER: AFWAL-TR-84-1032	2. GOVT ACCESSION NO.: AD-A148203
3. RECIPIENT'S CATALOG NUMBER	
4. TITLE *(and Subtitle)*: CHARACTERIZATION OF III-V COMPOUND SEMICONDUCTOR DEVICE MATERIALS	5. TYPE OF REPORT & PERIOD COVERED: Final Report for period Oct 1979- Oct 1983
	6. PERFORMING ORG. REPORT NUMBER
7. AUTHOR(s): D. C. Reynolds	8. CONTRACT OR GRANT NUMBER(s)
9. PERFORMING ORGANIZATION NAME AND ADDRESS: Air Force Avionics Laboratory, AF Wright Aeronautical Laboratories, AFSC, Wright-Patterson Air Force Base, Ohio 45433	10. PROGRAM ELEMENT, PROJECT, TASK AREA & WORK UNIT NUMBERS: 2306R101
11. CONTROLLING OFFICE NAME AND ADDRESS: Air Force Avionics Laboratory AFWAL/AADR, AF Wright Aeronautical Laboratories, AFSC, Wright-Patterson Air Force Base, Ohio 45433	12. REPORT DATE: May 1984
	13. NUMBER OF PAGES: 41
14. MONITORING AGENCY NAME & ADDRESS *(if different from Controlling Office)*	15. SECURITY CLASS. *(of this report)*: Unclassified
	15a. DECLASSIFICATION/DOWNGRADING SCHEDULE

16. DISTRIBUTION STATEMENT *(of this Report)*

Approved for public release; distribution unlimited.

17. DISTRIBUTION STATEMENT *(of the abstract entered in Block 20, if different from Report)*

18. SUPPLEMENTARY NOTES

19. KEY WORDS *(Continue on reverse side if necessary and identify by block number)*

GaAs
III-V Semiconductor
Photoluminescence
Transport measurements
Local Vibrational mode

20. ABSTRACT *(Continue on reverse side if necessary and identify by block number)*

The objective of this task has been the electrical, optical, and magneto-optical characterization of the intrinsic and extrinsic properties of compound semiconductors, primarily from the III-V group of materials. Photoluminescent techniques were used to identify both the intrinsic and extrinsic properties of the materials. Intrinsic properties such as energy band gaps, effective mass parameters, refractive indices, dielectric functions, exciton binding energies, and lattice vibration frequencies were determined. Extrinsic properties including activation energies of foreign impurites, binding

DD FORM 1 JAN 73 1473 EDITION OF 1 NOV 65 IS OBSOLETE

Unclassified

SECURITY CLASSIFICATION OF THIS PAGE *(When Data Entered)*

energy of excitons to foreign impurities and the energies of complexes were established. Transport measurements were used to measure carrier mobilities and electrical conductivity as well as carrier concentrations. These measurements as a function of temperature make it possible to determine the number of donors (N_D) and the number of acceptors (N_A) and therefore the compensation ratio in the material. Local vibrational mode spectroscopy was used as a characterization tool to identify specific impurities such as C and S_i in GaAs. From the vibrational energy the site location of the impurity can be determined. These characterization techniques have been very successful in evaluating the quality of materials and have been very helpful to the crystal growing program which has been successful in growing very high quality materials.

FOREWORD

This report covers the work performed under Task 2306R101, from 1 October 1979 to 1 October 1983. The objective of this task is to completely characterize the electronic impurity and defect structure of III-V semiconductors, including selected ternary and quaternary compounds. Emphasis is given to characterization of residual impurities, native defects, impurity dopants, and concentration profiles in high purity and doped epitaxial layers and meltgrOwn substrate crystals. The homogeneity of impurities and lattice imperfections as well as the electronic defect structure at surfaces and interfaces of these materials is also investigated. A major part of the effort is devoted to impurity and defect characterizations in GaAs and InP materials required for high frequency microwave and opto-electronic devices such as diodes, power sources, high power FET's, digital processing systems, laser diodes, optical light guides, and infrared detectors.

The principal contributors to the task effort during its existence were the following:

D. C. Reynolds, Task Manager

C. W. Litton, Research Scientist

E. B. Smith, Research Scientist

Most of the research has been reported in a series of papers published in the scientific literature; these are referenced at the end of each section. This research was performed at the Avionics laboratory, Air Force Wright Aeronautical Laboratories, Wright-Patterson Air Force Base, Ohio 45433.

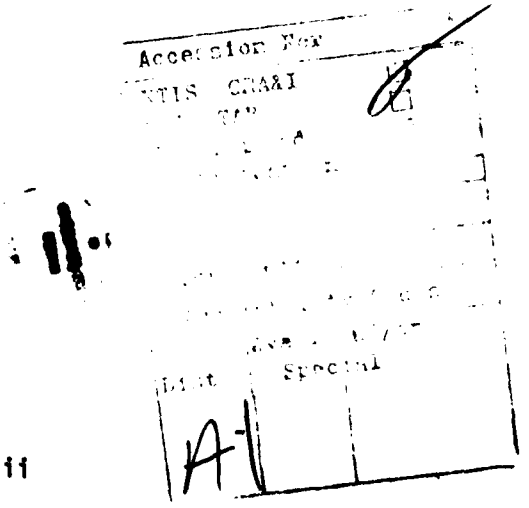

TABLE OF CONTENTS

LIST OF ILLUSTRATIONS

SECTION I

CHARACTERIZATION OF III-V COMPOUND SEMICONDUCTOR DEVICE MATERIALS

1. INTRODUCTION

Sophisticated characterization capabilities are essential in order to satisfactorily analyze high purity semiconductor materials. The electrical properties of semiconductors have a long history of extensive investigation. As the investigations of semiconductors were extended to wider band gap materials electrical measurements were not as readily applicable. This coupled with the understanding of excitons and their contribution to the elucidation of materials properties in the 1960's lead to a wide application of optical studies to semiconductor materials. It was found that these materials reflect, absorb, disperse, scatter and radiate light, and in general interact strongly with the electromagnetic radiation field. Because of this strong interaction many of the fundamental properties of these materials such as their energy band gaps, activation energies of defects and foreign impurities, effective mass parameters, refractive indicies, dielectric functions, exciton binding energies, and lattice vibration frequencies can be determined from optical experiments.

The technique of high resolution optical absorption, reflection, and photoluminescence spectroscopy has been extensively used to analyze the intrinsic energy band parameters of semiconductors, as well as their impurity and defect states. Intrinsic or free exciton formation is observed in most well formed crystal structures when optically excited with the proper energy and at cryogenic temperatures. The free excitons have been applied with a great deal of success in probing the intrinsic band structure of semiconductors. Bound excitons have been applied successfully in probing the impurity and defect structure of many of these same materials. The free exciton is the probe in this case, becoming bound to various chemical impurities, lattice defects and complexes to form bound states whose subsequent radiative decay yields information concerning the electronic states of the impurities and defects in these materials. Magnetic field splittings of the bound

exciton transitions make it possible to differentiate between neutral and ionized donor and acceptor impurities. In conjunction with systematic impurity doping experiments, specific donor and acceptor impurities can be identified. Upon application of stress fields, in conjunction with a knowledge of the energy band structure of the host lattice, it is also possible to differentiate between simple substitutional donors and acceptors and complexes comprising combinations of impurities and/or defects.

SECTION II

HIGH RESOLUTION OPTICAL AND MAGNETO-OPTICAL CHARACTERIZATION

1. OPTICAL CHARACTERIZATION

Reflection, emission, and absorption in solids has long been studied. Intense photoluminescence is observed in many semiconductors at low temperatures. When spectrally analyzed, this photoluminescence provides an extensive source of experimental data which contributed to the ultimate identification of the electronic states of impurities and defects in these semiconductors. Many sharp lines appear in such spectra, particularly from bound excitons, which provide a "finger print" of the impurities and defects which are present in the semiconductor lattice.

The exciton is the probe in this case, becoming bound to various impurities, defects, and complexes and the subsequent decay from the bound state yields information concerning the center to which it was bound. Early photoluminescent investigations were primarily centered on free to bound and bound to bound transitions such as the so called "edge emission" studies which gave rise to relatively broad emission. In the 1960's the effort shifted to more intensive studies of the sharp-line emission, aimed at identifying the bound exciton impurity transitions and at achieving a better understanding of the residual impurity and defect structure of semiconductors which have application in the electronic industry. The magnetic field splittings of these sharp line transitions make it possible to differentiate between neutral and ionized donor and acceptor impurities. In conjunction with systematic impurity doping experiments, specific donor and acceptor impurities may be identified.

The behavior of these sharp line transitions in perturbing magnetic and strain fields make it possible to differentiate between simple substitutional donors and acceptors and complexes composed of combinations of impurities and or defects.

The electrical properties of semiconductors has a long history of extensive investigation. Many of the basic properties of these materials

were determined from electrical measurements. As the investigations of semiconductors were extended to some of the larger band gap materials, electrical measurements were not as readily applicable. This coupled with the understanding of excitons and their contribution to the elucidation of material properties in the 1960's lead to a wide application of optical studies to semiconductor materials. It was found that these materials reflect, absorb, disperse, scatter, and radiate light and in general interact strongly with the electromagnetic radiation field. Because of this strong interaction many of the fundamental properties of these materials such as their energy band gaps, activation energies of defects and foreign impurities, effective mass parameters, refractive indicies, dielectric functions, exciton binding energies, and lattice vibration frequencies can be determined from optical experiments. These experiments cover the electromagnetic spectrum, ranging from the vacuum ultraviolet to the far infrared. Over the past two decades, optical spectroscopy has been increasingly employed for the study and measurement of semiconductor properties and has ultimately become a very powerful experimental tool.

The technique of high resolution optical absorption, reflection, and photoluminescence spectroscopy has been extensively used to analyze the intrinsic energy band parameters of semiconductors, as well as their impurities and defect states. Intrinsic or free exciton formation is observed in a most well formed crystal structure when optically excited with the proper energy and at cryogenic temperatures. The free excitons have been applied with a great deal of success in probing the intrinsic band structure of semiconductors. Bound excitons have been applied equally successfully in probing the impurity and defect structure of many of these same materials.

2. INTRINSIC EXCITON SPECTRA AND BAND STRUCTURE

The intrinsic fundamental gap exciton in semiconductors is a hydrogenically bound hole-electron pair, the hole being derived from the top valence band and the electron from the bottom conduction band. It is a normal mode of the crystal created by an optical excitation wave, and its wave functions are analogous to those of the Block wave states

of free electrons and holes. When most semiconductors are optically excited at low temperatures it is the intrinsic excitons that are excited. The energy of the ground and excited states of the exciton lie below the band gap energy of the semiconductor. Hence, the exciton structure must first be determined in order to determine the band gap energy. The exciton binding energy can be determined from spectral analysis of its hydrogenic ground and excited state transitions. Precise bandgap energies can be determined by adding the exciton binding energy to the experimentally measured photon energy of the ground state transition.

Both direct and indirect exciton formation occurs in semiconductors, depending on the band structure. The latter is characteristic of germanium and silicon. For indirect optical transitions, momentum is conserved by the emission or absorption of phonons. The detailed nature of the valence band structure of degenerate and nondegenerate semiconductors is elucidated by understanding the intrinsic exciton structure of these semiconductors.

3. NONDEGENERATE SEMICONDUCTORS

Nondegenerate semiconductors are typified by those materials that belong to the wurtzite crystal structure. This is a uniaxial structure belonging to the C_{6V} crystal space group. The early detailed studies of the intrinsic exciton spectra of crystals having this structure were concentrated on the II-VI wurtzite class of semiconductors, the first work being done on CdS.

A detailed study of the absorption edge of CdS in the temperature range 90-340 K was made by Dutton (Reference 1). The dichroism reported by Gobrecht and Bartschat (Reference 2) and also by Furlong and Ravilious (Reference 3) was clearly demonstrated. Dutton was unable to account for the source of the dichroism but felt that the absorption near the edge was due to exciton transitions. Gross and co-workers (References 4-6) studied the absorption near the edge on CdS at 4.2 K. They attributed the short-wavelength intrinsic absorption lines to exciton transitions. Birman (Reference 7) attacked the problem from a theoretical point of view. Assuming a tight binding approximation in conjunction with group theory, he arrived at the irreducible representations, band symmetries,

and selection rules for the wurtzite structure. If one considers the absorption (emission) of electromagnetic radiation by atoms, and probability of the occurrence of a transition between two unperturbed states Ψ_i and Ψ_f as caused by the interaction of an electromagnetic radiation field and a crystal is dependent on the matrix element

$$\int \Psi_f^* H_{int} \Psi_i \, dr \tag{1}$$

where H_{int} is the dipole moment operator

$$H_{int} = \frac{e\hbar}{imc} A \cdot \nabla \tag{2}$$

In order for an electric dipole transition to be allowed, the above matrix element between the initial and final states must be nonzero.

In the case of transitions between two states of an atom (which is in a crystalline field), the initial and final states of the atom are characterized by irreducible representations of the point group of the crystal field. Also the dipole moment operation must transform like one of the irreducible representations of the group. If one denotes the representations which correspond to the initial and final states of the transition and to the multipole radiation of order S(S = 0 for electric dipole radiation) Γ_i, Γ_f, and $\Gamma_r(s)$, respectively at k = 0, then the matrix element in Equation 1 transforms under rotations like the triple direct product

$$\Gamma_f \times \Gamma_r^{(s)} \times \Gamma_i \tag{3}$$

The selection rules are then determined by which of the triple products in question do not vanish.

The dipole moment operator for electric dipole radiation transforms like x, y, or z, depending on the polarization. When the electric vector ξ of the incident light is parallel to the crystal axis, the operator corresponds to the Γ_1 representation. When it is perpendicular to the crystal axis, the operator corresponds to the Γ_1 representation.

In the tight binding approximation, the wave functions at the center of the Brillouin zone are taken to be linear combinations of atomic wave functions. In CdS it is assumed that the bottom of the conduction band is formed from the 5s levels of Cd, and the upper valence bands are formed from the 3p levels of sulfur. Since the crystal has a principal axis, the crystal field removes part of the degeneracy of the p levels. Thus, disregarding spin-orbit coupling, the following decomposition at the center of the Brillouin zone is obtained:

conduction band $S \rightarrow \Gamma_1$

$P_x, P_y \rightarrow \Gamma_5$

valence band $P_z \rightarrow \Gamma_1$

Introducing the spin doubles the number of levels. The splitting caused by the presence of spin is represented by the inner products

$$\Gamma_5 \times D_{1/2} \rightarrow \Gamma_7 + \Gamma_9$$

$$\Gamma_1 \times D_{1/2} \rightarrow \Gamma_7$$

and the band structure at k = 0 along with the band symmetries and selection rules is shown in Figure 1. This band structure could readily account for the dichroism observed in CdS and other wurtzite-type structures.

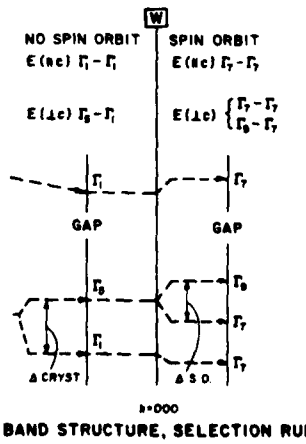

Figure 1. Band Structure and Selection Rules for the Wurtzite Structure. Crystal splittings and spin-orbit splittings are indicated schematically. Transitions which are allowed for various polarization of photon electric vector with respect to crystal c axis are indicated (Reference 7).

4. DEGENERATE SEMICONDUCTORS

Materials that crystallize in the diamond or the zinc blende structures are representative of degenerate semiconductors. Two materials that have been extensively investigated and are characteristic of direct degenerate semiconductors are GaAs and InP. These materials crystallize in the zinc blende structure which has Td^2 space group symmetry.

The dipole movement operator for electric dipole radiation in zinc blende structures transforms like Γ_4. The conduction band is S-like while the valence band is P-like. This structure does not have a principal axis, therefore, the crystal field energy is zero and the full degeneracy of the P-levels is retained. Thus, disregarding spin orbit coupling, the following decomposition at the center of the Brillouin zone is obtained:

Conduction band S $\rightarrow \Gamma_1$

Valence band P $\rightarrow \Gamma_4$

Introducing the spin doubles the number of levels. Consider the Γ_1 S-like conduction band and the triply degenerate P-like valence band. The states at the center of the Brillouin zone, which belong to Γ_1 and Γ_4 representations of the single group, are shown in Figure 2. The splitting caused by the presence of spin is represented by the inner product as follows:

$$\Gamma_1 \times D_{1/2} \rightarrow \Gamma_6$$

$$\Gamma_4 \times D_{3/2} \rightarrow \Gamma_7 + \Gamma_8$$

Physically this result means that the six valence band states, consisting of the three P-like states each associated with one or the other of the two spin states, and which are degenerate in the absence of spin-orbit interaction, now split into two levels one having Γ_7 symmetry and the other having Γ_8 symmetry. The Γ_8 level is fourfold degenerate while the Γ_7 level is twofold degenerate. In atoms, it is known that the fourfold degenerate state $P_{3/2}$ has greater energy than the doubly degenerate $P_{1/2}$ state. It is also known that the greatest contribution

to the spin-orbit energy comes from the atom core therefore, it is likely that the splitting in crystals will be similar to that in atoms. This would result in the Γ_8 level lying above the Γ_7 level as shown in Figure 2.

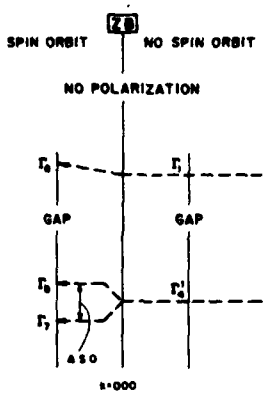

BAND STRUCTURE, SELECTION RULES, ZB

Figure 2. Band Structure for the Zinc Blende Crystal Structure. Spin-orbit splitting is indicated schematically (Reference 7).

5. DIRECT EXCITONS IN DEGENERATE SEMICONDUCTORS

The direct exciton at (K = 0) is formed by an electron in the conduction band of symmetry Γ_6 (J = 1/2) and a hole in the valence band of symmetry Γ_8 (J = 3/2). Excitons formed in this way will have the symmetries $(\Gamma_6 \times \Gamma_8) = \Gamma_3 + \Gamma_4 + \Gamma_5$.

The j - j coupling scheme results in two excitons one with total effective spin j = 1 and the other with effective spin J = 2. The J = 1 and J = 2 exciton states are split in zero field due to the electron hole exchange energy. The J = 1 states are optically allowed in zero

field; the J = 2 states are not. When a magnetic field is present, the J = 2 states may be optically allowed due to the mixing between the states of $|J = 2, M_j = \pm 1, 0\rangle$ and $|J = 1, M_j = \pm 1, 0\rangle$. This is shown for the case of GaAs in Figure 3.

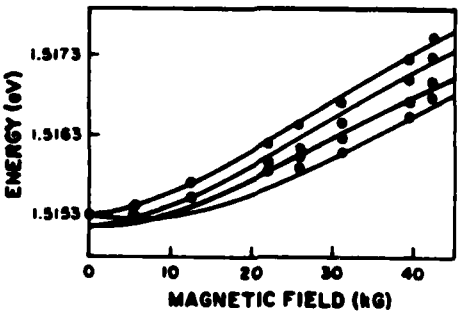

Figure 3. Energy of the Ground State Free Excitons in GaAs as a Function of Magnetic Field -, Calculated Values (Reference 17).

A great deal of interest as well as considerable effort has been devoted to understanding the free-exciton energy spectrum of zinc-blende-type semiconductors (References 8-18). This work has included both theoretical and experimental investigations both in zero field and with an external magnetic field applied. The ground states of the free exciton have been rather extensively investigated, however, the excited states of the free exciton have not received as much attention. The two materials from which the greatest amount of data have been recorded are GaAs and InP.

6. EXTRINSIC EXCITON SPECTRA

Bound exciton complexes or impurity exciton complexes are extrinsic properties of materials. These complexes are observed as sharp line optical transitions in both photoluminescence and absorption. The bound complex is formed by binding a free exciton to a chemical impurity atom (ion), complex, or a host lattice defect. The binding energy of the exciton to the impurity or defect is generally weak compared to the free exciton binding energy. The resulting complex is molecular-like (analogous

to the hydrogen molecule or molecule-ion) and bound excitons have many spectral properties which are analogous to those of simple diatomic molecules. The center to which the free excitons are bound can be either neutral donor and acceptor centers or ionized donor and acceptor centers. The emission or absorption energies of these bound exciton transitions are always below those of the corresponding free exciton transitions due to the molecular binding energy.

The sharp spectral lines of bound exciton complexes can be very intense (large oscillator strength). The line intensities will, in general, depend on the concentrations of impurities and/or defects present in the sample.

The theory of "impurity" or defect absorption intensities in semiconductors has been studied by Rashba (Reference 19). By use of the Fredholm method (Reference 20), he finds that, if the absorption transition occurs at k=0 and if the discrete level associated with the impurity approaches the conduction band, the intensity of the absorption line increases. The explanation offered for this intensity behavior is that the optical excitation is not localized in the impurity but encompasses a number of neighboring lattice points of the host crystal. Hence, in the absorption process, light is absorbed by the entire region of the crystal consisting of the impurity and its surroundings.

In an attack on the particular problem of excitons which are weakly bound to localized "impurities", Rashba and Gurgenishvili (Reference 21) derived the following relation between the oscillator strength of the bound exciton F_d and the oscillator strength of the intrinsic excitons f_{ex}, using the effective-mass approximation

$$F_d = (E_0/|E|)^{3/2} f_{ex} \qquad (4)$$

where $E_0=(2h^2/m)(\pi/\Omega_0)^{3/2}$, E is the binding energy of the excitation to the impurity, m is the effective mass of the intrinsic exciton, and Ω_0 is the volume of the unit cell.

It has been shown in some materials that F_d exceeds f_{ex} by more than four orders of magnitude. An inspection of Equation 16 reveals that, as the intrinsic exciton becomes more tightly bound to the associated

center, the oscillator strength, and hence the intensity of the exciton complex line, should decrease as $\left(\frac{1}{|E|}\right)^{3/2}$.

In magnetic fields, bound excitons have unique Zeeman spectral characteristics, from which it is possible to identify the types of centers to which the free excitons are bound. Bound exciton spectroscopy is a very powerful analytical tool for the study and identification of impurities and defects in semiconductor materials. It has been employed rather extensively over the last few years for the characterization of materials, many of which have been used in practical device applications such as solid state lasers, light emitting diodes, and a variety of microwave devices.

It is convenient to describe the details of bound excitons in relation to the particular crystal lattice which provides their environment.

7. ACCEPTORS AND DONORS IN GaAs

The shallow acceptors in GaAs have binding energies approximately five times larger than the donor binding energies. The larger binding energies have permitted accurate determination of the binding energies of the different shallow chemical acceptors. The acceptor energies were optically characterized by Ashen, et al. (Reference 22) using bound exciton transitions as well as free to bound transitions. The energies they obtained are given in Table 1.

The shallow donors in GaAs have been considerably more difficult to characterize. From high-resolution, Fourier transform infrared (FTIR) magneto-spectrographic studies, which employed the modulated photoconductivity detection technique to monitor the $1s \rightarrow 2p_{-1}$ transitions of isolated hydrogenic donors in a fixed magnetic field, Stillman, et al. (Reference 23) have detected three residual donors in high purity vapor phase epitaxial (VPE) GaAs, while Stradling, et al. (Reference 24) have found the same number of residual donors in liquid phase epitaxial (LPE) material. Wolfe and coworkers (References 25, 26) have performed similar

TABLE 1

ENERGIES OF SPECTRAL LINES IN GaAs

Acceptor	Observed Free-to-Bound Transition (5K) (eV ± 0.3 meV)	Bound Exciton (1S) (1.5 doublet) Centre) (eV ± 0.05 meV)	Binding Energy $1S_{3/2}$ (Ground State) (meV)
Carbon	1.4935	1.5124_2	26.0
Silicon	1.4850	1.5123_5	34.5
Germanium	1.4790	1.5126_6	40.4
Tin	1.349	1.5067_7	171
Zinc	1.4888	1.5122_8	30.7
Cadmium	1.4848	1.5123_2	34.7
Beryllium	1.4915	1.5124_0	28.0
Magnesium	1.4911	1.5124_0	28.4

spectral measurements in conjunction with back-doping experiments in VPE GaAs and have identified one of the residual donors as silicon on the gallium site (hereafter denoted as X_2). The other two residual donors (denoted as X_1 and X_3) could not be given a definite chemical identification; however, it was suggested that X_3 was probably due to carbon on a gallium site (Reference 26) and speculated that X_1 might have arisen from a native defect, possibly a Ga-vacancy (References 25, 26). Following a procedure similar to that of Wolfe and coworkers, Ozeki, et al. (Reference 27) have attempted to identify the residual donors in VPE GaAs. Their assignments, however, differ from those of Wolfe, et al.

(Reference 26); moreover, the binding energy of the silicon donor they measure is smaller than that determined by Wolfe, et al. (Reference 26). Recently Afsar (Reference 28) and co-workers have initiated a systematic effort to identify the residual donors in VPE GaAs by means of FTIR magneto-spectroscopy performed over a wide range of high magnetic fields. Their preliminary results indicate that X_2 and X_3 are due to silicon and germanium, respectively. Recently, Almassy, et al. have investigated the radiative transitions associated with donor exciton complexes. A typical region is displayed in Figure 4. The line D_1, arises from unresolved radiative recombination of excitons bound to neutral donors in which the donors are left in their ground states.

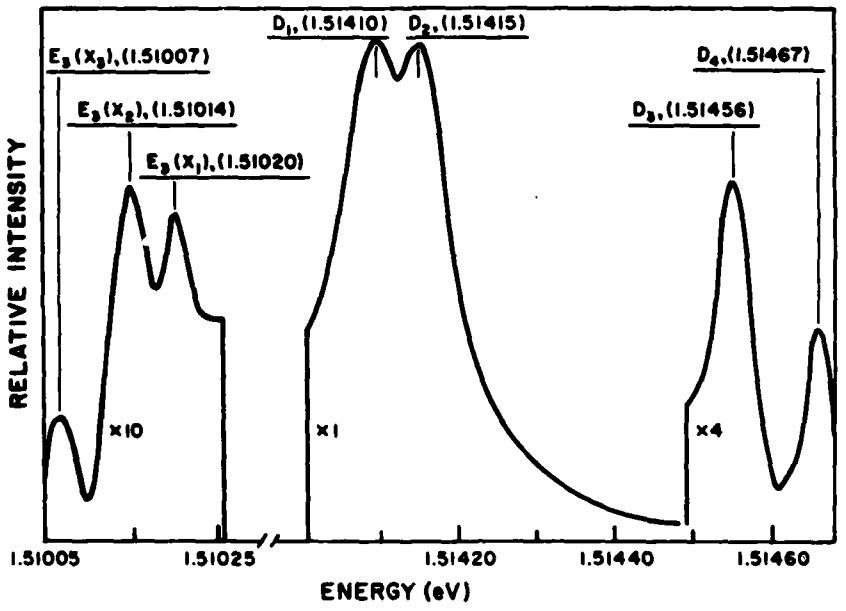

Figure 4. Typical Photoluminescence Spectrum of High Purity VPE GaAs in the Near Band Edge Region at ~2 K. The origin of the various displayed transitions is explained in the text.

Since the differences between the binding energies of different donors in GaAs are very small (the maximum spread in the binding energies of donors is at most 0.2 meV) it is not possible to resolve such transitions which arise from the recombination of excitons bound to different donors. Thus, if only one donor were present, the peak marked D_1 would represent the resolved transition of that donor to its ground state. It has been suggested that the lines marked D_2, D_3, and D_4 arise from radiative recombination of excitons bound to one or more neutral donors for the case where the resulting donor exciton complex is initially in excited states, but it is not possible to calculate accurately the energies of these states. Energies of such states have, however, been estimated (Reference 29) by invoking a non-rigid rotator model as an approximation to the donor exciton complex, a model in which these states are identified with the low-lying rotational states of such system. The energies thus obtained agree fairly well with observed values.

Thomas and Hopfield (Reference 30) observed transitions from bound exciton states in CdS that were characterized by large magnetic field splittings and negative diamagnetic shifts. They tentatively identified these transitions as resulting from the collapse of a bound exciton which leaves the terminal state in an excited state. Subsequently a number of such transitions have been observed and identified (References 31,32,33-38).

The origin of the line marked $E_3(X_1)$ and on the lower-energy-side of the D peaks, is attributed to such a mechanism. An exciton bound to a neutral donor recombines when the complex as a whole is in the D_3 excited state, leaving the donor electron in the first excited state of an isolated neutral donor, as shown in Figure 5. In this process, the emitted photon will have an energy which is equal to the energy of the D_3 line minus the energy of the above excitation. One can show from symmetry considerations (group theoretic arguments, in particular) that both the 2s and 2p states are allowed final states. However, the energies of the 2s and 2p states are so close to one another that it is not possible to resolve them experimentally. Excited state transitions corresponding to the complex in D_1 and D_2 excited configurations are also observed. But the associated excited state transitions due to different donors

(analogous to the D_3 mechanism denoted above) are much more difficult to resolve in the case of the D_1 and D_2 excited configurations, owing to the small separation between the D_1 and D_2 lines. If the final state of excitation of the donor electron is assumed to be 2s, the difference between D_3 and $E_3(X_1)$ is then the difference in energy between the 1s and 2s states of this donor. The binding energy of this donor can therefore be calculated using a value of the impurity Rydberg, $R_0^* = 5.737$ meV, (which incidentally includes a contribution due to parabolicity of the conduction band).

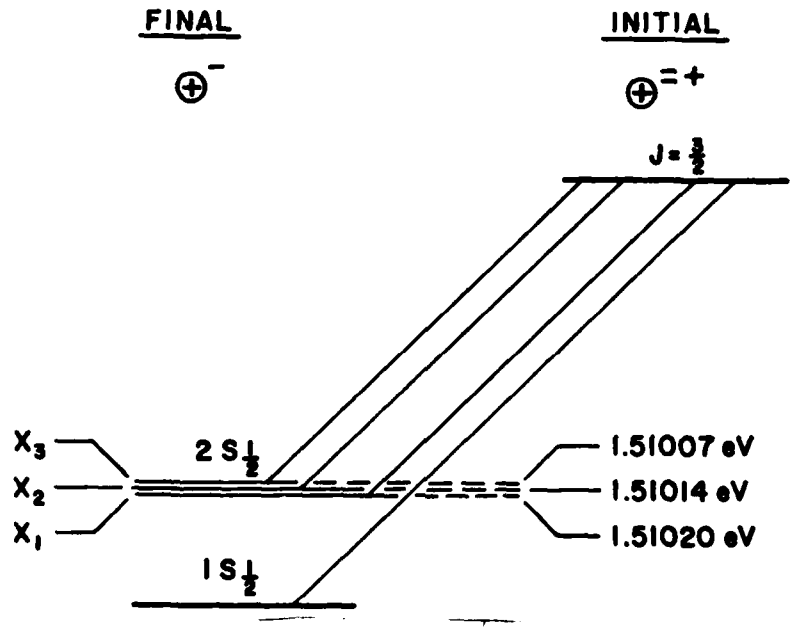

Figure 5. Schematic Representation of Radiative Recombination of an Exciton in the Exciton-Donor Complex where the Final State is the Donor in the Ground or in the Excited Configuration.

This value was deduced from careful high resolution FTIR spectroscopic measurements of the $1s \rightarrow 2p_{-1}$ transition of an isolated donor (Reference 23). Central cell correction to the 2s state is assumed to be 1/8 of its value for the 1s state. The lines marked $E_3(X_2)$ and $E_3(X_3)$ arise from similar transitions due to two other donors. From an analysis of the spectral data, the binding energies of all three donors were calculated

and are presented in Table 2, where the transitions $E_3(X_1)$, $E_3(X_2)$ and $E_3(X_3)$ are assigned to the previously designated X_1, X_2 and X_3 donors, respectively. For comparison the values of the binding energy of these donors as measured by two other groups using high-resolution FTIR magneto-spectroscopy are shown. Although slightly larger, the values obtained by Almassy, et al. agree rather well with those obtained by other groups.

TABLE 2

BINDING ENERGIES OF RESIDUAL DONORS IN VPE GaAs (UNITS OF meV)

Donor Designation	Measurement: Wolfe, et al. (5) (FTIR)	Measurement: Ozeki, et al. (6) (FTIR)	Measurement: Present Results (Photoluminescence)
X_1	5.801	5.795	5.804
X_2	5.854	5.845	5.870
X_3	5.937	5.949	5.978

If it is assumed that the final state of the donor is 2p rather than 2s, then the values of the binding energy obtained by Almassy, et al. for all three donors are identical to those of Wolfe, et al. (Reference 26). The values of Ozeki, et al. (Reference 27) are quite close to those of the other two groups, except that their chemical assignments for these donors are different. As mentioned earlier, Ozeki, et al. assign X_1 to silicon whereas Wolfe, et al. (Reference 26) and Cooke, et al. (Reference 39) and recently Afsar, et al. (Reference 28) assign X_2 to silicon. In addition, Wolfe, et al. and Cooke, et al. assign X_3 to carbon whereas Ozeki, et al. and Afsar, et al. assign X_3 to germanium. The donor X_1 has not been chemically identified by any other group except by Ozeki, et al. The samples used in the study made by Almassy, et al. were not intentionally doped, therefore it was not possible to propose

chemical identifications of the residual donors. The characterization technique does however offer another approach to the problem of identifying residual donors in GaAs.

It should be pointed out that due to the extreme sharpness of bound exciton transitions and the use of a high resolution (~.007 meV) spectrograph, the excited state transitions due to different residual donors are very well resolved. On the other hand, high-resolution Fourier transform spectroscopic measurements require the application of fairly high magnetic fields to resolve transitions due to different donors in VPE GaAs and further require a theoretical analysis of the data in order to derive the binding energies at zero field.

8. DONOR-ACCEPTOR TYPE COMPLEXES

Donor-acceptor pair spectra have been observed in a number of materials and are readily recognized by the complex line spectra that results. Reynolds, et al. (Reference 40) have observed six different emission lines in GaAs each of which behaves like a donor-acceptor type complex. They combined strain patterns and magnetic field splittings with their photoluminescent studies to aid in identifying these transitions. One of these lines (1.51165 eV) will be discussed here.

The uniaxial strain patterns and electric dipole selection rules were derived for lines arising from weakly bound exciton complexes in uniaxially strained zinc-blende semiconductors by Bailey (Reference 44). The effect of stress on excitons bound to shallow neutral acceptors in GaAs was investigated by Schmidt, et al. (Reference 42).

In the unstrained crystal, a hole from the J = 3/2 (Γ_8) valence band in combination with an electron from the J = 1/2 (Γ_6) conduction band gives rise to the ground-state exciton. Uniaxial stress splits the J = 3/2 degenerate valence band into two bands--one with $M_j = \pm 3/2$, the other with $M_j = \pm 1/2$. This splitting is reflected in optical transitions involving holes from the valence band. The shallow acceptor removes an energy state from the valence band and establishes it as a quantum state of lower energy in the gap region. This state is made up to valence-band wave functions and therefore will also reflect valence-band splittings.

A crystal, with grown-in strain, was produced that showed splitting in both the neutral donor-bound exciton lines and the neutral-acceptor-bound exciton lines. The strain-field behavior of the acceptor-bound exciton lines and the complex line is shown in Figure 6. From the line splitting of the shallow acceptor-bound exciton as shown in Figure 6 the local stress was determined using the calibrated measurement of Schmidt, et al. (Reference 42). The measured value of local stress from Figure 6 is as great as 0.3 kG mm^{-2}. From this observation they gained vital information concerning the nature of the complex giving rise to the 1.51165 eV line. It was not associated with an exciton transition since the hole component of the exciton is derived from the valence band and would therefore show the strain splitting. Therefore, a bound exciton complex could be ruled out. A free to bound transition could also be ruled out, first because the line is much narrower than the calculated kT broadening and second the energy position of the line would require that the transition go from a free hole to a bound electron. The hole would therefore reflect the valence-band splitting which is not observed experimentally. The line must therefore arise from a bound-to-bound transition, from a donor to an acceptor state or vice versa.

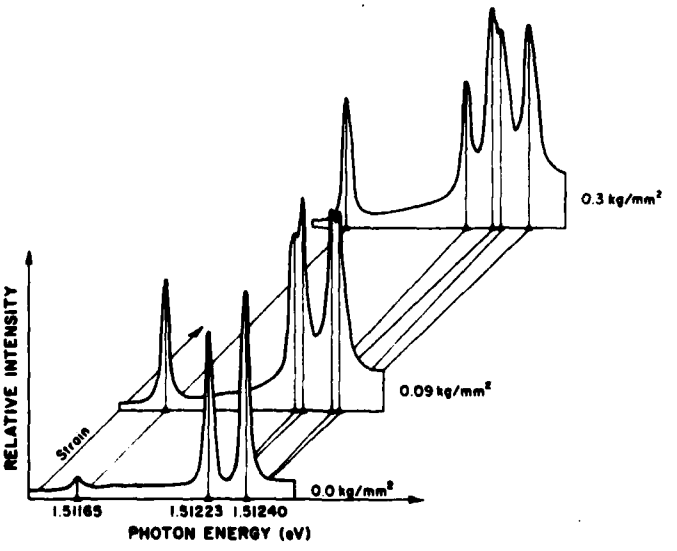

Figure 6. Strain-Field Behavior of the Acceptor-Bound-Exciton Lines as Well as the Donor-Acceptor-Type Complex Line at 1.51165 eV (Reference 40).

The linear magnetic field splitting of the line at 1.51165 eV is shown in Figure 7. In this figure, the photon-energy deviation from the spectral center of mass is plotted as a function of the magnetic-field strength. The large magnitude and the linearity of the magnetic-field splitting is evident. Assuming that the initial state of this transition is a J = 3/2 state and the final state is a J = 1/2 state, or vice versa, and electron g-value of $g_e = -0.35 \pm 0.15$ and a hole of value $\kappa = 2.01 \pm 0.11$ were obtained. This value of κ is large compared to the value $\kappa = 1.0 \pm 0.2$ obtained from studies of the free exciton as well as $\kappa = 0.51 \pm 0.15$, from bound exciton complexes in the same energy region. The g-value of the electron is comparable to the value $g_e = -0.50 \pm 0.05$ deduced from the free-exciton spectrum and the calculated value of $g_e = -0.48$ (Reference 17).

The analysis of the magnetic-field-split lines is dependent on the detailed nature of the complex. Three different donor-acceptor complexes are shown in Figure 8. In Figure 8a, the double acceptor-neutral donor complex is shown schematically. The initial state of the complex is quite complicated; two holes and a single electron combine to give three states in zero magnetic field with angular momentum J = 5/2, J = 3/2, and J = 1/2. Each of these states will split in a magnetic field. The final state consists of a J = 3/2 hole which will also split in a magnetic field. The behavior of such a complex could be expected to be quite similar to the behavior of an acceptor-bound exciton. Figure 8b shows the double donor-neutral acceptor complex. The upper state consists of two paired electron spins and an unpaired J = 3/2 hole state that will split in an externally applied magnetic field. The lower state consists of an electron which will contribute a spin splitting in a magnetic field. The neutral donor - neutral acceptor complex is shown in Figure 8c. In this complex the upper state consists of a single electron and a single hole resulting in two states in zero field, depending on the spin orientation of the hole and electron, with angular momentum J = 2 and J = 1. Both of these states will split in a magnetic field.

Reynolds, et al. used a geometric construction to analyze the line at 1.5116 as shown in Figure 9. The densitometer trace shows the relative intensity of the lines. The double acceptor-donor, Figure 8a, involves

a complex initial state which would be expected to yield three observable lines in zero field. The magnetic-field splitting of the 1.51165 eV line shows a sixfold multiplicity, suggesting that the transition occurs between J = 3/2 and J = 1/2 states. For the model of the double acceptor-neutral donor to explain the data, it would require that only the J = 1/2 upper state contribute. Schairer, et al. (Reference 43) describe conditions where this might occur. The upper state would then be a Kramers doublet which would not split in a strain field. The lower state would be the

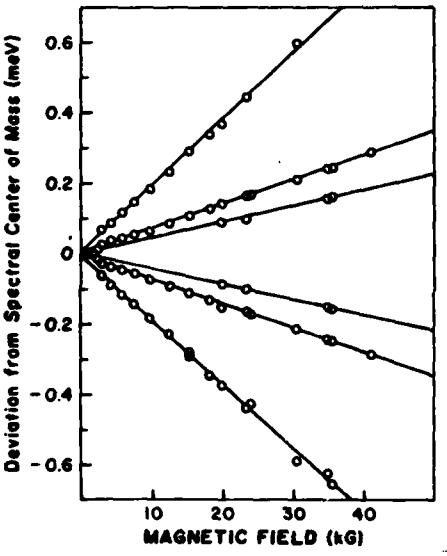

Figure 7. The Linear Magnetic Field Splitting of the Donor-Acceptor Complex (Reference 40).

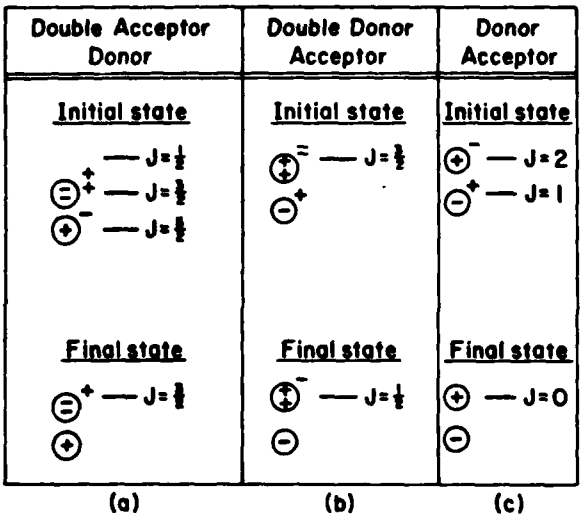

Figure 8. Representative Donor-Acceptor-Type Complexes: (a) Double-Acceptor-Donor, (b) Double-Donor-Acceptor, (c) Donor-Acceptor (Reference 40).

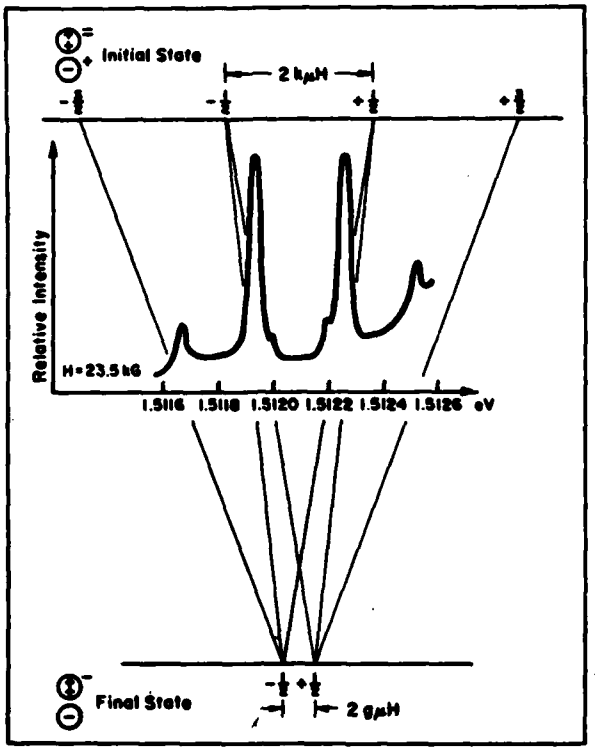

Figure 9. Zeeman Spectrum of the 1.51165-eV Line at 23.5-kG Applied Magnetic Field. A nomogram for interpretation of the lines is included.

single-hole state of the double acceptor. This would be a deep level that would not reflect the valence-band splitting. It would be expected that the neutral donor-neutral acceptor type complex shown in Figure 8c would have a zero-field splitting due to the exchange energy. The acceptor involved in the complex must be relatively deep. If it were shallow it would show strain splitting analogous to that observed in the shallow-bound exciton complexes. The greater binding energy of the acceptor should contribute to a greater exchange splitting. Since no zero field splitting was observed, they ruled out the neutral donor-neutral acceptor complex. The remaining double donor-acceptor complex shown in Figure 8a can account for all of the experimental data provided the acceptor is deep. Therefore, the model of the double acceptor-neutral donor with the constraint that only the J = 1/2 upper state contributes,

or the double donor-deep neutral acceptor can account for the experimental observations. The origin of the double acceptor or double donor is quite likely an antisite defect (Reference 44). Arsenic on a gallium site would produce a double donor, whereas gallium on an arsenic site would produce a double acceptor. The origin of the neutral donor or neutral acceptor was not determined. This experiment is further evidence of the usefulness of photoluminescent experiments in identifying impurities and defects in crystals. Details of the results of high resolution optical and magneto-optical characterization on this task are described in the following journal articles:

1. K. K. Bajaj and C. H. Aldrich, "Theory of Excitons in Cubic Semiconductors in Arbitrary Magnetic Fields: Application to GaAs," Solid State Commun. 35, 163 (1980).

2. K. K. Bajaj, T. D. Clark, and W. M. Theis, "Ground-State Energy of a Donor Bound Exciton Complex in Semiconductors," Proc. 15th Int. Conf. on Physics of Semiconductors, Kyoto (Japan), 1980; J. Phys. Soc. Japan 49 (1980), Suppl. A457.

3. W. M. Theis, C. W. Litton, and K. K. Bajaj, "Infrared Localized Vibrational Mode Spectroscopy of Carbon-Implanted GaAs," SPIE Vol. 276, Optical Characterization Techniques for Semiconductor Technology (1981), p. 109.

4. T. D, Clark, K. K. Bajaj, W. M. Theis, and D. E. Phelps, "Theory of Donor-Bound Exciton Complexes in Semiconductors," Physica Status Solidi (b) 110, 341 (1982).

5. D. E. Phelps and K. K. Bajaj, "Screening Effects on the D^- System in Semiconductors," Phys. Rev. B26, 912 (1982).

6. W. M. Theis, K. K. Bajaj, C. W. Litton, and W. G. Spitzer, "Direct Evidence for the Site of Substitutional Carbon Impurity in GaAs," Applied Physics Letters, 41, 70 (1982).

7. D. E. Phelps and K. K. Bajaj, "Effect of Free Carrier Screening on the Binding Energy of D^- Centers in Polar Semiconductors," Solid State Commun. 45, 121 (1983).

8. G. B. Norris and K. K. Bajaj, "The Exciton-Plasma Mott Transition in Silicon," Phys. Rev. B26, 6706 (1982).

9. D. E. Phelps and K. K. Bajaj, "Effect of Screening Due to Free Mobile Charges on the Binding Energy of an H^- Ion," The Astrophysical Journal, 268, 447 (1983).

10. W. M. Theis, K. K. Bajaj, C. W. Litton, and W. G. Spitzer, "Direct Evidence for the Site of Substitutional Carbon Impurity in GaAs Using Localized Model Vibrational Spectroscopy," Proc. 16th Int. Conf. on The Physics of Semiconductors, Montpellier, France, 6-10 Sep 82, Physica 117B and 118B, 116 (1983).

11. R. L. Greene and K. K. Bajaj, "Energy Levels of Hydrogenic Impurity States in GaAs-GaAlAs Quantum Well Structures," Solid State Commun. 45, 825 (1983).

12. R. L. Greene and K. K. Bajaj, "Binding Energies of Wannier Excitons in GaAs-GaAlAs Quantum Well Structures". Solid State Commun. 45, 831 (1983).

13. D. E. Phelps and K. K. Bajaj, "Ground-State Energy of a D^- Ion in Two-Dimensional Semiconductors" Phys. Rev. B27, 4883 (1983).

14. R. L. Greene and K. K. Bajaj, "Energy Levels of Hydrogenic Impurities and Wannier Excitons in Quantum Well Structures," J. Vac. Sci. Technol. B1(2) 391, 1983.

15. D. C. Reynolds and C. W. Litton, "Semiconductor Materials Characterization by High-Resolution Optical Spectroscopy," Society of Photo-Optical Instrumentation Engineers 276, 11 (1981).

16. D. C. Reynolds, C. W. Litton, E. B. Smith, and K. K. Bajaj, "Photoluminescence Studies of Exciton-Ionized Donor Complexes in High Purity Epitaxial GaAs," Solid State Commun. 44, 47 (1982).

17. P. C. Colter, D. C. Look, and D. C. Reynolds, "Low Compensation Vapor Phase Epitaxial Gallium Arsenide," Appl. Phys. Lett., 43, 282 (1983).

18. P. C. Colter, D. C. Reynolds, C. W. Litton, and E. B. Smith, "Identification of the Tellurium Donor at the Residual Level in GaAs," Solid State Commun. 45, 375 (1983).

19. D. C. Reynolds, C. W. Litton, E. B. Smith, K. K. Bajaj, T. C. Collins, and M. H. Pilkuhn, "Radiative Transitions with Two-Acceptor-One-Donor Complexes in Epitaxial GaAs and InP," Phys. Rev. B, 28, 1117 (1983).

20. R. J. Almassy, D. C. Reynolds, C. W. Litton, K. K. Bajaj, and G. L. McCoy, "Observation of Shallow Residual Donors in High Purity Epitaxial GaAs by Means of Photoluminescence Spectroscopy," Solid State Commun. 38, 1053 (1981).

21. D. C. Reynolds, K. K. Bajaj, C. W. Litton, and E. B. Smith, "Identification of Residual Donors in High-Purity Epitaxial GaAs with the Use of Magneto-Optical Spectroscopy," Phys. Rev. B, 28, 3300 (1983).

22. D. C. Reynolds, D. W. Langer, C. W. Litton, G. L. McCoy, and K. K. Bajaj, "Intensity-Reversal in the Donor Bound Exciton Luminescence of GaAs," Solid State Commun. 46, 473 (1983).

23. D. C. Reynolds, C. W. Litton, R. J. Almassy, and G. L. McCoy, "Complexes Due to Donor-Acceptor-Type Transitions in GaAs," J. Appl. Phys. 51, 4842 (1980).

24. D. C. Reynolds, C. W. Litton, E. B. Smith, P. W. Yu, and K. K. Bajaj, "Photoluminescence Studies of the Amphoteric Behavior of Carbon and Germanium in GaAs," Solid State Commun. 42, 827 (1982).

25. G. S. Pomrenke, D. C. Reynolds, and Y. S. Park, "Near-Edge Emission of Unimplanted and Mg-Implanted VPE InP," J. of Luminescence 24/25, 189 (1981).

SECTION III

TRANSPORT MEASUREMENTS

1. INTRODUCTION

Resistivity and Hall effect measurements are an integral part of the semiconductor characterization process and thus their use is widespread. For conductive materials ($\rho \lesssim 10\Omega$) both the required apparatus and the measurement procedures are quite simple. In recent years, however, the interest in semi-insulating high resistivity ($\rho \lesssim 10^7 \Omega$cm) GaAs and InP substrate materials has greatly increased, as well as the need for investigating these materials (Reference 45). Other important semiconductors also exhibit very high resistivity. Apparatus has been constructed which can automatically measure high or low resistivity and Hall coefficients, as well as their dependences upon temperature, magnetic field, and monochromatic light wavelength and intensity. These measurements provide information concerning the conductivity type, carrier mobility, carrier concentration, and compensation ratio of the samples investigated. The energy position of impurity and defect levels can also be obtained. These data are essential to a comprehensive characterization effort.

2. TRUE MOBILITIES IN SEMI-INSULATING, OXYGEN AND CHROMIUM DOPED GaAs

It is well known that an analysis of the magnetic field dependencies of the resistivity ρ and Hall coefficient R, in nearly intrinsic material, will uniquely yield the electron mobility μ_n, the hole mobility μ_p, the electron concentration n, and the hole concentration p as long as single-carrier magnetic field dependences are not important. Unfortunately, recent data indicate that such effects are often important in semi-insulating GaAs and thus a new approach was necessary. The problem was treated by using an approach that required only the usual, low field Hall effect and resistivity parameters, R_o and ρ_o, but that also assumed knowledge of the intrinsic carrier concentration N_i, and the hole mobility as a function of the electron mobility, i.e., $\mu_p = f(\mu_n)$. The analyses yielded $N_i \approx (2.6 \pm 0.5) \times 10^6$ cm^{-3}, and a tentative relationship for μ_p

namely, $\mu_p^{-1} \simeq 9x10^{-4} + 13\ \mu_N^{-1}$. Curves for μ_N versus R_o/ρ_o, with ρ_o as a parameter were calculated by using the above relationships. For $\rho_o \leq 4x10^8 \Omega cm$, the only solutions were $\mu_n \simeq R_o/\rho_o$ which means that simple Hall measurements are adequate for nearly all oxygen doped and undoped semi-insulating GaAs. For higher ρ_o the solutions are double-valued and thus a scheme was provided for selecting the proper solutions. A simple compensation-distribution model was used to determine the positions of the oxygen and chromium energy levels.

3. A DOMINANT ELECTRICAL DEFECT IN GaAs

It has long been known that defects can lead to electrically active centers in semiconductors, such as GaAs. However, it has never been shown that a "pure" defect, not associated with any chemical impurity, can dominate the electrical properties of any as-grown crystal. Such a situation would have important implications for any device technology associated with that material. In the past, shallow donor impurities (in particular silicon) have dominated bulk GaAs. Recently, however, as crystal growers have been able to reduce silicon contamination, we have seen an increasing number of as-grown Bridgman and Czochralski GaAs crystals controlled by levels from 0.13 to 0.20 eV below the conduction band. These crystals were studied by the temperature-dependent Hall-effect, spark-source mass spectroscopy, and secondary-ion mass spectroscopy. It was shown that no impurity was of sufficient concentration to account for these levels, and therefore they are composed of single or multiple defects. The detailed nature of the defects has not yet been established but may involve an arsenic vacancy. This is the first time that a dominant electrically active center has been shown to be a pure defect in any as-grown semiconductor.

4. A DETAILED SEMI-INSULATING GaAs SUBSTRATE STUDY: CONVERSION AND MESFET PROPERTIES

A detailed investigation of 21 SI GaAs substrates, Cr-doped, O-doped, and undoped, Bridgman and Czochralski, from eight different manufacturers, has been carried out by temperature-dependent Hall effect (TDH), differential Hall effect (DH), photoluminescence (PL), spark-

source mass spectroscopic (SSMS), and secondary-ion mass spectroscopic (SIMS) measurements. Also, Si-ion-implanted MESFET's, with 4 μm gates, were fabricated on several of the substrates and tested. Electrical conversion tests were carried out to simulate typical VPE growth conditions (750^{o}C, 15 min, H_2 atmos., no cap), and ion-implantation annealing conditions (900^{o}C, 15 min, H_2 atmos., Si_3N_4 cap). The following conclusions have emerged from this study: (1) It is very difficult to get reliable n-type activation at less than the mid-10^{17} cm^{-3} level, at least with 120 keV Se ions. (2) Low mobilities ($\lesssim 10^3$ cm^2/V-sec), often seen in SI GaAs substrate materials, are due to inhomogeneity (if $\rho \lesssim 4 \times 10^8$ Ω-cm). The effective channel mobilities in implanted MESFET's, near pinch-off, are heavily influenced by these low substrate mobilities. (3) The commonly observed 0.5 eV acceptor conversion level is due to Fe, but the 0.1 eV acceptor level is <u>not</u> always due to Mn, as evidently believed by many workers.

5. STATISTICS OF MULTICHARGE CENTERS IN SEMICONDUCTORS

A general formula was derived for the electron occupation numbers appropriate for multicharge centers in semiconductors, including excited states. The results were used to rederive and generalize several formulas of interest in the literature in order to show exactly how the degeneracies of individual states enter in. Particular attention was paid to certain subjects which are sometimes confusing, such as how the statistics of band states differ from those of localized states. Another subject of much recent interest, negative-U centers was dealt with in some detail. It was shown how the dependence of the average occupation number on Fermi energy and the temperature dependence of the free-carrier concentration differ between positive- and negative-U centers.

6. MAGNETO-HALL AND MAGNETORESISTANCE COEFFICIENTS IN SEMICONDUCTORS WITH MIXED CONDUCTIVITY

Magneto-Hall and magneto-resistance formulas, correct to order B^2, were derived for the case in which both single-carrier and mixed-carrier effects are important. Also, a new magneto-Hall coefficient is presented: $\beta = \langle\tau^4\rangle\langle\tau\rangle^z_{2f}/\langle\tau^2\rangle^3 - 1$. Values of β for various scattering mechanisms were calculated and compared with experiment.

7. PHOTOLUMINESCENCE AND OTHER RELATED TECHNIQUES

Photoluminescence, combined with other optical techniques such as absorption, photoconductivity, photo-induced transient current spectroscopy, and local-mode spectroscopy, were used for the assessment of semiconducting materials. Information leading to band parameters and extrinsic properties can be detected without destruction of the samples, which makes the photoluminescence technique suitable for both substrate and multilayer materials. The variation of temperature, uniaxial stress, magnetic field, excitation intensity and wavelength helps to identify the parameters involved in the device elements. The physical parameters which can be determined from photoluminescence are the following: (a) band parameters; (b) uniformity of multilayer structures; (c) impurity and defect levels; (d) the nature of intrinsic defects and defect-complexes; (e) lifetimes of radiative recombination; and (f) the symmetry of defects and their electronic states. Details of the results of transport measurements on this task are described in the following journal articles:

1. D. C. Look, "Resonance Photoconductivity in Fe-doped InP," Sol. State Commun. 33, 237 (1980).

2. J. W. Farmer and D. C. Look, "Electron Irradiation Defects in n-Type GaAs," Phys. Rev. B21, 3389 (1980).

3. D. C. Look, J. W. Farmer and R. N. Ely, "Automation of a Popular Monochromator," Rev. Sci. Instr. 51, 968 (1980).

4. D. C. Look, "True Mobilities in O- and Cr-doped GaAs," Semi-Insulating III-V Materials Conf., ed. by G. J. Rees (Shiva, Orpington, 1980) p. 183.

5. D. C. Look and J. W. Farmer, "Automated, High-Resistivity Hall-Effect and Photoelectronic Apparatus," J. Phys. E. Sci. Instrum. 14, 472 (1981).

6. D. C. Look, "The Statistics of Multi-Charge Centers in Semiconductors: Application," Phys. Rev. B 24, 5582 (1981).

7. D. C. Look, "The Electrical and Photoelectronic Properties of Semi-Insulating GaAs," Vol 19 of Semiconductors and Semimetals (ed. by R. K. Willardson and A. C. Beer).

8. D. C. Look, "Magneto-Hall and Magnetoresistance Coefficients in Semiconductors with Mixed Conductivity," Phys. Rev. B B25, 2920 (1982).

9. D. C. Look, D. C. Walters, and J. R. Meyer, "A Dominant Electrical Defect in GaAs," Solid State Commun. 42, 745 (1982).

10. D. C. Look and G. S. Pomrenke, "A Study of the 0.1 eV Conversion Acceptor in GaAs," J. Appl. Phys. 54, 3249 (1983).

11. D. C. Look, P. W. Yu, J. E. Ehret, Y. K. Yeo, and R. Kwor, "A Detailed SI GaAs Substrate Study: Conversion and MESFET Properties," in Semi-Insulating III-V Materials, Evian, 1982; ed. by S. Makram-Ebeid and B. Tuck (Shiva, Nantwich, U.K.), 1982, p. 372.

12. D. C. Look, S. Chaudhuri, and L. Eaves, "Positive Identification of the Cr^{4+} Cr^{3+} Thermal Activation Energy in GaAs," Phys. Rev. Lett. 49, 1728 (1982).

13. D. C. Look, L. Chaudhuri, and J. R. Sizelove, "Defect Nature of the 0.4 eV Center in O-doped GaAs," Appl. Phys. Lett. 42, 829 (1983).

14. H. J. Lee and D. C. Look, "Hole Transport in Pure and Doped GaAs," J. Appl. Phys. 54, 4446 (1983).

15. S. Chaudhuri and D. C. Look, "Effect of the Velocity-Field Peak on I-V Characteristics of GaAs FET's," Solid State Electronics 26, 811 (1983).

16. D. C. Look and P. C. Colter, "Electrical Properties of Low-Compensation GaAs," Phys. Rev. B28, 1151 (1983).

17. P. W. Yu, "A Model for the 1.10-eV Emission Band in InP," Solid State Commun. 34, 183 (1980).

18. P. W. Yu, "Photoluminescence and Photoconductivity Study of the 1.10-eV Energy Level in Fe-doped InP," Semi-Insulating III-V Materials Conference, Nottingham, April, 1980.

19. D. W. Covington, J. Comas, and P. W. Yu, "Iron Doping in Gallium Arsenide by Molecular Beam Epitaxy," Appl. Phys. Lett. 37, 1094 (1980).

20. D. E. Holmes, R. G. Wilson, and P. W. Yu, "Redistribution of Fe in InP During Liquid Phase Epitaxy," J. Appl. Phys. 52, 3396 (1981).

21. P. W. Yu, "Iron in Heat-Treated Gallium Arsenide," J. Appl. Phys. 52, 5786 (1981).

22. J. R. Oliver, R. D. Fairman, R. T. Chen, and P. W. Yu, "Undoped Semi-Insulating LEC GaAs," Elect. Lett. 171, 839 (1981).

23. P. W. Yu and D. C. Reynolds, "Photoluminescence Identification of 77meV Deep Acceptor in GaAs," J. Appl. Phys. 53, 1263 (1982).

24. P. W. Yu, D. E. Holmes, and R. T. Chen, "Photoluminescence Study in LEC GaAs," in Gallium Arsenide and Related Compounds - 1981, edited by T. Sugano, IOP Conf. Proc. No. 63 (IOP, Bristol and London, 1982), p. 209.

25. P. W. Yu, "Deep Center Photoluminescence in Undoped Semi-Insulating GaAs: 0.68-eV Band Due to the Main Deep Donor," Solid State Commun. 43, 953 (1982).

26. P. W. Yu and D. C. Walters, "Deep Photoluminescence Band Related to Oxygen in GaAs," Appl. Phys. Lett. 41, 863 (1982).

27. P. C. Colter, C. W. Litton, D. C. Reynolds, D. C. Look, P. W. Yu, S. S. Li, and W. L. Wang, "Novel Ga/$AsCl_3/H_2$ Reactor for Controlling Stoichiometry in the Growth of Vapor Phase Epitaxy GaAs," Proceedings of SPIE, 323, Semiconductor Growth Technology, 28 (1982).

28. D. E. Holmes, R. T. Chen, K. R. Elliot, C. G. Kirkpatrick, and P. W. Yu, "Compensation Mechanism in Liquid Encapsulated Czochralski GaAs," IEEE MTT-30, 949 (1982).

29. P. W. Yu, "Studies on the 0.58-eV Photoluminescence Emissions in Heat-Treated Semi-Insulating GaAs," in Semi-Insulating III-V Materials, ed. by Ebeid and Tuck (Shiva Publishing Limited, 1982), p. 305.

30. P. W. Yu, W. C. Mitchel, M. G. Mier, S. S. Li, and W. L. Wang, "Evidence of Intrinsic Double Acceptor in GaAs," Appl. Phys. Lett. 41, 532 (1982).

31. P. W. Yu, "Photoluminescence Excitation of the 1.441-eV Cation Antisite Emission in p-Type GaAs," Phys. Rev. B27, 7779 (1983).

REFERENCES

1. Dutton, D., Phys. Rev. 112, 785 (1958).

2. Gobrecht, H., and Bartschat, A., Z. Phys. 136, 224 (1953).

3. Furlong, L. R., and Ravilious, C. F., Phys Rev. 98, 954 (1955).

4. Gross, E. F., Nuovo Cimento Suppl. 3, 672 (1956).

5. Gross, E. F., Razbirin, B. S. and Jakobson, M., Zh. Tekhn Fiz. 27, 1149 (1957).

6. Gross, E. F., and Razbirin, B. S., Zh. Tekhn Fiz. 27, 2173 (1957) (English transl.: Sov. Phys. Tech. Phys. 2, 2014 (1957).

7. Birman, J. L., Phys. Rev. Lett. 2, 157 (1959); J. Phys. Chem. Solids 8, 35 (1959); Phys. Rev. 114, 1490 (1959).

8. Sell, D. D., Dingle, R., Stokowski, S. E., and Dilorenzo, J. V., Phys. Rev. Lett. 27, 1644 (1971).

9. Sell, D. D., Stokowski, S. E., Dingle, R., and Dilorenzo, J. V., Phys. Rev. B7, 4568 (1973).

10. Sell, D. D., Phys. Rev. B6, 3750 (1972).

11. White, A. M., Dean, P. J., Taylor, L. L., Clarke, R. C., Ashen, D. J., and Mullin, J. B., J. Phys. C5, 1727 (1972).

12. Dingle, R., Phys. Rev. B8, 4627 (1973).

13. Dreybrodt, W., Willmann, F., Bettini, M., and Bauser, E., Solid State Commun. 12, 1217, (1975).

14. Willman, F., Suga, S., Dreybrodt, W., and Cho, K., Solid State Commun. 14, 783 (1974).

15. Hill, D. E., Solid State Commun. 11, 1187 (1972).

16. Shay, J. L., and Nahory, R. E., Solid State Commun. 7, 945 (1969).

17. Nam, S. B., Reynolds, D. C., Litton, C. W., Almassy, R. J., Collins, T. C., and Wolfe, C. M., Phys. Rev. B13, 761 (1976).

18. Nam, S. B., Reynolds, D. C., Litton, C. W., Collins, T. C., and Dean, P. J., Phys. Rev. 13, 1643 (1976).

19. Rashba, E. I., Opt Spektrosk. 2, 508 (1957).

20. Lovit, W. V., Linear Integral Equations, 1st ed. Dover, New York 1950.

REFERENCES (Cont'd)

21. Rashba, E. I. and Gurgenishvili, G. E., Fiz. Tverd. Tela 4, 1029 (1962) (English transl.: Sov. Phys. Solid State 4, 759 (1962).

22. Ashen, D. J., Dean, P. J., Hurle, D. T., Mullin, J. B., and White, A. M., J. Phys. Chem. Solids 36, 1041 (1975).

23. Stillman, G. E., Larsen, D. M., Wolfe, C. M., and Brandt, R. C., Solid State Commun. 9, 245 (1971).

24. Stradling, R. A., Eaves, L., Hoult, R. A., Miura, N. Simmonds, P. E., and Bradley, C. C., Gallium Arsenide and Related Compounds (Inst. Phys. Conf. Ser. 17) 65, 1972.

25. Wolfe, C. M., Korn, D. M., and Stillman, G. E., Appl. Phys. Lett. 24, 78 (1974).

26. Wolfe, C. M., Stillman, E. G., and Korn, D. M., Gallium Arsenide and Related Compounds (Inst. Phys. Conf. Ser. 33b) 120, 1977.

27. Ozeki, M., Kitahara, K., Nakai, K., Shibatomi, A., Dazai, K., Okawa, S., and Ryuzan, O., Jap. J. Appl. Phys. 16, 1617 (1977).

28. Afsar, M. N., Button, K. J., and McCoy, G. L., Int. J. of Infrared and Millimeter Waves 1, 145 (1980).

29. Rhule, W. and Klingenstein, W., Phys. Rev. B12, 7011 (1978).

30. Thomas, D. G. and Hopfield, J. J., Phys Rev. 128, 2135 (1962).

31. Rossi, J. A., Wolfe, C. M., Stillman, G. E., and Dimmock, J. O., Solid State Commun. 8, 2021 (1970).

32. Merz, J. L., Kukimots, H., Nassau, K., and Shiever, J. W., Phys. Rev. 6B, 545 (1972).

33. Dean, P. J., Cuthbert, J. D., Thomas, D. G., and Lynch, R. T., Phys. Rev. Lett. 18, 548 (1967).

34. Reynolds, D. C., Litton, C. W., and Collins, T. C., Phys. Rev. 174, 845 (1968); Phys. Rev. 177, 1161 (1969).

35. Reynolds, D. C. and Collins, T. C., Phys. Rev. 185, 1099 (1969).

36. Nassau, K., Henry, C. H., and Shiever, J. W., (Proc. X Int. Conf. Phys. Semicond. Cambridge MA) 629, (1970).

37. Reynolds. D. C., Litton, C. W., Collins, T. C., Nam, S. B., and Wolfe, C. M., Phys. Rev. 12, 5723 (1975).

REFERENCES (Concluded)

38. Reynolds, D. C., Litton, C. W., Almassy, R. J., Nam, S. B., and Dean, P. J., Phys. Rev. 13, 2507 (1976).

39. Cooke, R. A., Hoult, R. A., Kirkman, R. F., and Stradling, R. A., J. Phys. D. Appl. Phys. 11, 945 (1978).

40. Reynolds, D. C., Litton, C. W., Almassy, R. J., and McCoy, G. L., J. Appl. Phys. 51, 4842 (1980).

41. Bailey, P. T., Phys. Rev. B1, 588 (1970).

42. Schmidt, M., Morgan, T. N., and Schairer, W., Phys. Rev. B11, 5002 (1975).

43. Schairer, W., Bomberg, D., Kottler, W., Cho, K., and Schmidt, M., Phys. Rev. B13, 3452 (1976).

44. Van Vechten, J. A., J. Electrochem. Soc. 122, 423 (1975).

45. Look, D. C., J. Appl. Phys. 48, 5141 (1977).

END

FILMED

1-85

DTIC